Desalination and Water Treatment
www.deswater.com
doi: 10.1080/19443994.2013.770191

51 (2013) 5574–5582
August

Taylor & Francis
Taylor & Francis Group

Adsorption characteristics of copper(II) onto non-crosslinked and cross-linked chitosan immobilized on sand

Kuo-Jung Hsien[a], Cybelle M. Futalan[b], Wan-Chi Tsai[c], Chi-Chuan Kan[d] Chun-Shuo Kung[d], Yun-Hwei Shen[a], Meng-Wei Wan[d,*]

[a]*Department of Resources Engineering, National Cheng Kung University, Tainan, Taiwan 701, Republic of China*
[b]*Department of Environmental Engineering, University of Philippines-Diliman, Quezon City 1800, Philippines*
[c]*Department of Medical Laboratory Science and Biotechnology, Kaohsiung Medical University, Kaohsiung, Taiwan 80708, Republic of China*
[d]*Department of Environmental Engineering and Science, Chia Nan University of Pharmacy and Science, Tainan Taiwan 71710, Republic of China*
Tel. +88 66 266 0615; Fax: +88 66 213 1291; email: peterwan@mail.chna.edu.tw

Received 16 May 2012; Accepted 9 December 2012

ABSTRACT

In this study, Cu(II) removal using non-crosslinked and cross-linked chitosan-coated sand (CCS) from aqueous solution was investigated. To improve the mechanical and chemical stability, chitosan was coated onto sand (CCS) and cross-linked using epichlorohydrin (ECH) and ethylene glycol diglycidyl ether (EGDE). The effect of pH (2.0–5.0) on the adsorption capacity was examined. The maximum adsorption capacity of CCS, CCS–ECH, and CCS–EGDE occurred at an initial pH of 5.0, 4.0, and 5.0, respectively. The kinetic experimental data agreed well with pseudo-second order equation ($R^2 > 0.988$), which implies that chemisorption is the rate controlling step. Langmuir, Freundlich and Dubinin–Radushkevich were used to analyze the equilibrium data, where the Langmuir model provided the best fit for the isotherm data obtained using CCS, CCS–ECH, and CCS–EDGE ($R^2 > 0.990$). Adsorption-desorption was carried out using HCl solution (pH 1.0 and 3.0) and tap water (pH 7.0), where HCl solution (pH 1.0) provided the greatest recovery of Cu(II) at 98.3, 87.5 and 83.5% for CCS, CCS–ECH and CCS–EDGE, respectively. The removal of Cu(II) from real groundwater samples were studied, where removal of 57.4, 62.4 and 77.5% were achieved using CCS, CCS–ECH and CCS–EDGE.

Keywords: Crosslinking; Chitosan; Desorption; Groundwater; Isotherm

1. Introduction

Occurrence of heavy metals such as copper in groundwater and surface waters is due to natural weathering processes, atmospheric depositions, and industrial emissions. Several anthropogenic sources that produce copper in waste effluents include electroplating, brass fabrication, fungicide manufacturing, mining, and smelting [1]. Copper, Cu(II), is considered to be one of the essential trace elements needed by the human body. However, ingestion at high dosages could be detrimental to health, causing gastrointestinal

*Corresponding author.

disturbance, lesions in the central nervous system, Wilson's disease, liver, and kidney failure [2].

Current removal technologies, which are of physicochemical in nature, include chemical precipitation, ion exchange, flocculation, electrodeposition, and membrane filtration. These methods prove to be expensive due to high maintenance and operation costs, as well as ineffective in removing heavy metals in trace quantities [3]. Adsorption is an attractive method due to its ability in heavy metal removal from waste effluents with high solute loadings or trace quantities (<100 mg L^{-1}), ease of handling and operation, and cost-effectiveness [4,5]. Commercialized adsorbents such as activated carbon are widely used due to its high capacity in removing contaminants [6]. However, it remains an expensive material with complicated preparative and regeneration method, which led to the search for alternative low-cost adsorbents such as montmorillonite [1], chitin, and chitosan [7], banana pith [8], spent activated clay [9], wastewater sludge [10], peat [11], and pineapple leaf powder [12].

Chitosan, a low acetyl substituted form of chitin, is composed of glucosamine, 2-amino-2-deoxy-β-glucose units. It contains two types of functional groups: the amine group located at C-2 and hydroxyl groups found at C-3 and C-6 position [8]. The amine and hydroxyl groups of chitosan make physical and chemical modification possible. Physical modification includes spreading of chitosan onto an immobilized support, causing a decrease in crystallinity and expansion of porous network that leads to easy accessibility of the binding sites. On the other hand, chemical modification is applied to enhance chemical stability of chitosan in acidic media and decrease its solubility in most mineral and organic acids [7,13].

Silica sand is formed through natural weathering of quartzite and sandstone, where it is used in separation and purification processes due to its abundance, low cost, and porosity. Silica sand is composed of silica tetrahedral layer with hydroxyl groups found at the silicate structure edges [14]. Previous studies have affirmed the use of chitosan-coated sand (CCS) on copper and lead removal from aqueous solution [15]. However, there is very little research on cross-linked CCS on the adsorption of copper, where physical and chemical modifications would be applied in combination. This study would determine the feasibility of cross-linked CCS to be used as a possible material in building large-scale filters of a permeable reactive barrier system in treating contaminated groundwater and acidic plumes.

In continuation with the previous work [15], this study investigated the removal of Cu(II) from aqueous solution using non-cross linked and cross-linked CCS. The effect of pH on percent (%) removal and adsorption capacity was examined. The kinetic experimental data were fitted using pseudo-first-order and pseudo-second-order equations. Isotherm models such as Langmuir, Freundlich, and Dubinin–Radushkevich equations were applied in examining the equilibrium data. Desorption study was performed in order to determine reusability of the adsorbents using tap water and HCl solution as eluents. The adsorption capacity of CCS in removing Cu(II) from real groundwater system was also examined.

2. Materials and method

2.1. Materials and equipment

Low-molecular-weight chitosan (75.0–85.0% deacetylation degree), epichlorohydrin (ECH) of 99.0% purity, and ethylene glycol diglycidyl ether (EGDE) of 50.0% purity were obtained from Sigma-Aldrich. NaOH (99.0% purity) and HCl (37.0% fuming) were purchased from Merck, while $CuSO_4$ was procured from Ridel-de Ha n. A reciprocal shaker bath (YIH Der BT350) was utilized in the batch experiments. The quantitative analysis of Cu(II) was performed using an inductively coupled plasma optical emission spectroscopy (ICP-OES Perkin Elmer DV 2000 series). A channel precision oven (DV452 220 V) was used for drying the adsorbent. The pH was measured using a pH meter HACH Sension 3. A hot plate (CORNING Stirrer/Hot Plate PC-420D) was utilized in the synthesis of the CCS.

2.2. Preparation of CCS

CCS was prepared in a similar method utilized by Wan et al. [15] CCS with particle size in the range of 0.35–0.71 mm was utilized throughout the study.

2.3. Preparation of cross-linked CCS

Chitosan (5 g) was dissolved in 5% (v/v) HCl and was stirred for 2 h under 300 rpm. Sand (100 g) with 4.578 mL of EGDE or 1.162 mL of ECH was added into chitosan solution. The mixture was stirred for 3 h at 55˚C upon addition of EGDE and stirred for 2 h at 45˚C upon addition of ECH. The mixture was neutralized using 1 N NaOH and filtered. The adsorbent beads were washed using deionized water, oven-dried at 65˚C for 24 h and sieved. The CCS beads cross-linked using ECH and EGDE were designated as CCS–ECH and CCS–EDGE, respectively.

2.4. Characterization of adsorbent

The surface morphology of CCS, CCS–ECH and CCS-EDGE was analyzed using scanning electron microscope (S-3000 N Hitachi) analyzer using tungsten filament running under vacuum of 1.33×10^{-6} mBar at 20.0 kV. The samples were coated with a thin layer of gold (10 nm) using a sputter coater. The average pore diameter and surface area were measured using GEMINI 2360, Micrometrics gas adsorption surface analyzer using Brunauer, Emmett and Teller multipoint technique. The adsorption-desorption isotherm was collected at 77 K using liquid N_2.

2.5. Effect of solution pH

The effect of initial solution pH (2.0–5.0) on the adsorption capacity of CCS, CCS–ECH, and CCS–EDGE in the removal of Cu(II) was investigated. The upper pH range was chosen on the basis of the solubility of Cu(II), where a pH greater than 5.0 would result in the precipitation of Cu(II) hydroxides. The solution pH was adjusted using 0.1 N NaOH or 0.1 N HCl. Flasks containing 30 mL Cu(II) solution and 2.5 g adsorbent were agitated using 50 rpm at 25°C in 12 h under varying initial concentration (100–1,000 mg L^{-1}). Samples were filtered and residual Cu(II) ions were analyzed at a wavelength of 213.597 nm using ICP-OES. The adsorption capacity, q_e (mg g^{-1}) at equilibrium is calculated using the following equation:

$$q_e = \frac{(C_0 - C_e)v}{m} \quad (1)$$

where v is the volume of Cu(II) solution (mL), m is the weight of the adsorbent (g), C_0 is the initial concentration of the metal ion (mg L^{-1}), C_e is the final or equilibrium concentration of metal ion (mg L^{-1}).

2.6. Kinetic study

Kinetic studies were performed using 2.5 g adsorbent in a 30 mL Cu(II) solution with initial concentration varying from 100 to 2000 mg L^{-1} at optimum pH. The flasks were agitated under 25°C at pre-determined time intervals.

2.7. Equilibrium isotherm study

Equilibrium studies were carried out using 2.5 g adsorbent beads in 30 mL Cu(II) solution with a contact time of 24 h at optimum pH under varying initial concentration (100–2000 mg L^{-1}) under 25°C.

2.8. Desorption study

In the desorption study, Cu(II)-loaded adsorbent was desorbed using 30 mL desorbing agent (tap water and HCl solution) and agitated at 50 rpm for 6 h. The Cu(II) concentration contained in HCl or tap water was analyzed. The percentage of desorption was calculated using:

$$\text{DP } (\%) = \left(\frac{c_d}{c_a}\right) \times 100 \quad (2)$$

where DP (%) is percentage of desorption, c_d and c_a are the concentration of metal ions desorbed and adsorbed (mg L^{-1}), respectively.

2.9. Adsorption study using groundwater

Real groundwater was obtained from a monitoring well located in Chia Nan University of Pharmacy and Science in Tainan, Taiwan. Groundwater was spiked with initial Cu(II) concentration of 5 mg L^{-1}. About 30 mL of Cu(II)-spiked groundwater was placed in an Erlenmeyer flask under varying adsorbent mass (0.02–2.5 g) and was agitated for 24 h using 50 rpm. The background values and composition of groundwater were measured and shown in Table 1.

The percent (%) removal of Cu(II) from groundwater can be calculated as follows:

Table 1
Background values and chemical properties of groundwater

Parameters	Values
pH	8.1
Conductivity (μS cm^{-1})	2,480
Eh (mV)	75
Dissolved oxygen (mg L^{-1})	1.4
Total organic carbon (mg)	23.04
Humic acid (mg L^{-1})	18.27
Ion species	
Chloride (mg L^{-1})	246
Sulfate (mg L^{-1})	34.1
Phosphate (mg L^{-1})	1.59
Potassium (mg L^{-1})	34.39
Calcium (mg L^{-1})	24.36
Sodium (mg L^{-1})	624.9
Heavy metals	
Iron (mg L^{-1})	0.51
Manganese (mg L^{-1})	0.15
Total arsenic (μg L^{-1})	11.93
Zinc (mg L^{-1})	0.88

$$\text{Percent } (\%) \text{ removal} = \left(\frac{C_0 - C_e}{C_0}\right) \times 100 \quad (3)$$

3. Results and discussion

3.1. Surface morphology

The SEM micrographs of CCS, CCS–ECH, and CCS–EDGE are shown in Fig. 1. Similar surface morphology was observed for CCS and CCS–ECH, where the surface is rough and covered with uneven ridges. However, CCS displays a more uneven surface area with shallow ridges, while CCS–ECH illustrates deep, uneven ridges.

However, the morphology of CCS–EDGE provides a more irregular and rough texture, where the surface is more porous and covered with more uneven cavities and ridges. The deeper, numerous cavities and ridges display a denser texture in comparison with CCS and CCS–ECH.

3.2. Surface area analysis

Physical properties such as pore size and surface area of CCS, CCS–EC, and CCS–EDGE were observed to change during physical and chemical modification. Coating of chitosan ($0.037\,m^2\,g^{-1}$) onto sand ($0.367\ m^2\,g^{-1}$) and crosslinking using ECH and EGDE increased the surface area of CCS ($0.398\ m^2\,g^{-1}$), CCS–ECH ($0.413\ m^2\,g^{-1}$), and CCS–EDGE ($0.424\ m^2\,g^{-1}$). The surface area of the modified adsorbents is greater than chitosan and slightly higher than sand. CCS–EDGE beads provided the highest surface area over CCS and CCS–ECH. According to IUPAC recommendation, total porosity of an adsorbent could be classified based on its average pore diameter (d): micropores ($d < 2\,nm$), mesopores ($2\,nm < d < 50\,nm$), and macropores ($d > 50\,nm$) [13]. The average pore diameter of CCS, CCS–ECH, and CCS–EDGE are 4.939, 3.875, and 5.931 nm, indicating that the adsorbents are mesoporous materials. The total pore volume of CCS, CCS–ECH, and CCS–EDGE are 0.015, 0.027, and $0.032\,cm^3\,g^{-1}$, respectively.

3.3. Effect of pH

Fig. 2 illustrated the adsorption of Cu(II) under different initial solution pH (2.0–5.0). The Cu(II) uptake was observed to decrease as the solution becomes more acidic, where the lowest adsorption of Cu(II) occurred at pH 2.0 for all three adsorbents.

In Fig. 2(a) and (b), a similar pattern was observed where CCS–EDGE and CCS have better adsorption capacity over CCS–ECH under the pH range studied. In general, CCS, CCS–ECH and CCS-EDGE showed an increase in adsorption capacity as the pH was increased from 2.0 to 5.0. In Fig. 2(c), CCS–EDGE showed to have the highest adsorption capacity over CCS and CCS–ECH. This implies that under high initial Cu(II) concentration of $1{,}000\,mg\,L^{-1}$, there are more binding sites available in CCS–EDGE while the binding sites of CCS and CCS–ECH are limited and are easily saturated by Cu(II) ions. In Fig. 2(a)–(c), adsorption capacity was observed to increase with increasing initial Cu(II) concentration from 100 to $1{,}000\,mg\,L^{-1}$. A high metal ion loading means a better concentration gradient, which is an important driving force that will help overcome the mass transfer resistance of the metal ions between the liquid and solid phases [2,15].

In acidic solution, the amine groups were protonated to become amino groups ($-NH_3^+$), which induces an electrostatic repulsive force toward approaching Cu(II). In addition, H^+ would compete for and reduce the number of amine groups available for Cu(II) binding [16]. Results indicated that the maximum adsorption capacity of CCS and CCS–EDGE occurred at an optimum pH of 5.0, while the maximum Cu(II) uptake of CCS–ECH took place at an initial solution pH of 4.0, which implies that the optimum pH occurs at pH 5.0 for CCS and CCS–EDGE and pH 4.0 for CCS–ECH.

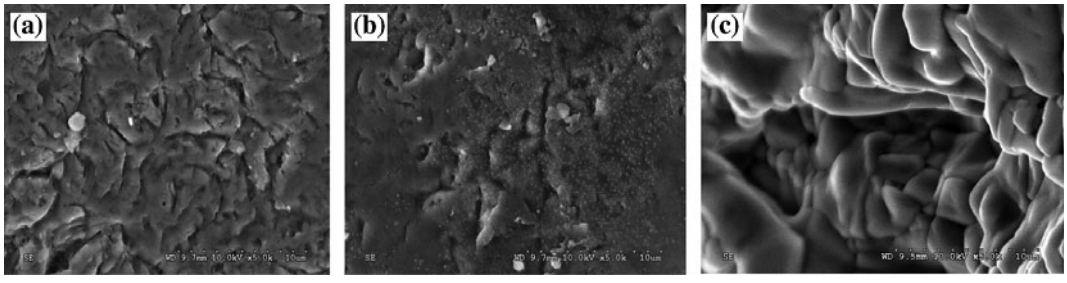

Fig. 1. SEM micrographs of (a) CCS, (b) CCS–ECH, and (c) CCS–EDGE.

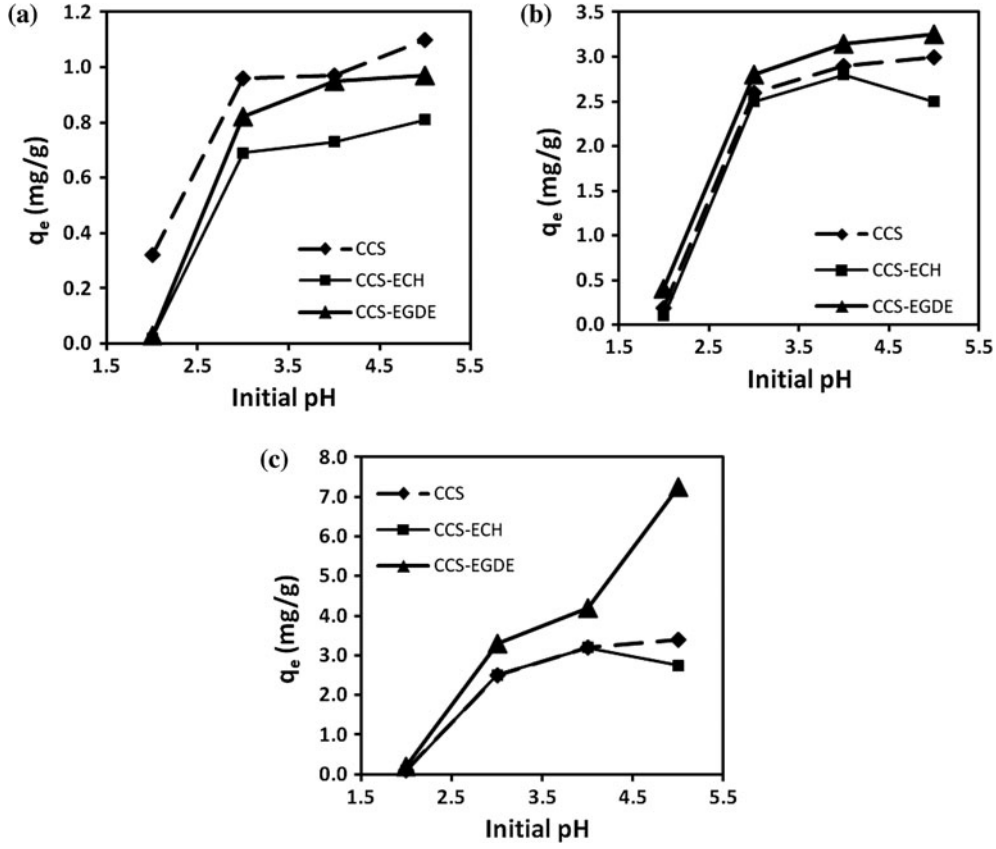

Fig. 2. Effect of initial pH on the adsorption capacity of CCS, CCS–ECH, and CCS–EDGE at an initial Cu(II) concentration of (a) 100 mg L^{-1}, (b) 500 mg L^{-1}, and (c) 1,000 mg L^{-1}.

3.4. Kinetic study

In order to estimate the rate of Cu(II) adsorption, pseudo-first-order and pseudo-second-order equation were applied to the kinetic experimental data. The pseudo-first-order or Lagergren equation is given as [17]:

$$\log(q_e - q_t) = \log q_e - \frac{k_1 t}{2.303} \quad (4)$$

where k_1 is the pseudo-first order rate constant, q_e is the adsorption capacity at equilibrium, and q_t is the adsorption capacity at time t.

The pseudo-second order model is presented as:

$$\frac{t}{q_t} = \frac{1}{k_2 q_e^2} + \frac{t}{q_e} \quad (5)$$

where k_2 is the pseudo-second-order rate constant [18,19].

Table 2 provides the information about the kinetic parameter constants, correlation coefficients of pseudo-first- and pseudo-second-order equation. The high coefficient of determination values ($R^2 > 0.988$) as well as the very good agreement between experimental and theoretical q_e data generated by pseudo-second-order equation validates that the kinetic data in the uptake of Cu(II) using CCS, CCS–ECH, and CCS–EDGE is best described by the pseudo-second-order equation. This implies that the rate-determining step is chemisorption, where covalent bonds are formed between Cu(II) and binding sites of the adsorbents. The values of pseudo-second-order rate constant, k_2 could be arranged in the following order: CCS > CCS–ECH > CCS–EDGE, which indicates that Cu(II) uptake was most rapid for CCS. The lower adsorption rate of CCS–ECH and CCS–EDGE indicated there is longer time for Cu(II) to diffuse along the adsorbent surface and into the pores, which led to more Cu(II) being adsorbed causing larger q_e values for CCS and CCS–EDGE. In comparison with CCS, the k_2 values of CCS–ECH and CCS–EDGE are larger, which could be attributed to its large surface area and pore volume.

3.5. Equilibrium study

Adsorption isotherms would provide information such as adsorption capacity, the affinity between Cu

Table 2
Kinetic parameters of Cu(II) adsorption onto CCS, CCS–ECH, and CCS–EDGE

Adsorbent	C_0 (mg L^{-1})	Experimental q_e (mg g^{-1})	Pseudo-first-order			Pseudo-second-order		
			k_1 (min^{-1})	$q_{e\ (theo)}$ (mg g^{-1})	R^2	k_2 g (mg min)$^{-1}$	$q_{e\ (theo)}$ (mg g^{-1})	R^2
CCS	100	1.04	0.015	0.945	0.968	0.039	1.289	0.996
	500	2.86	0.015	2.051	0.947	0.019	3.075	0.997
	1,000	3.67	0.019	1.438	0.750	0.039	3.924	0.999
	2,000	4.52	0.0138	2.786	0.960	0.019	5.732	0.999
CCS–ECH	100	0.86	0.014	0.642	0.986	0.026	0.922	0.999
	500	2.68	0.009	1.967	0.956	0.017	2.991	0.996
	1,000	4.02	0.009	3.673	0.986	0.007	4.641	0.988
	2,000	4.80	0.016	3.659	0.978	0.012	5.049	0.997
CCS–EDGE	100	0.81	0.001	0.675	0.944	0.023	1.077	0.994
	500	2.92	0.001	2.714	0.949	0.006	4.013	0.992
	1,000	4.50	0.011	3.855	0.961	0.007	4.929	0.997
	2,000	6.00	0.001	5.033	0.873	0.003	8.012	0.989

(II) and adsorbent, and bonding energy. The isotherm data of Cu(II) adsorption using CCS, CCS–ECH, and CCS–EDGE were analyzed using Langmuir, Freundlich, and Dubinin–Radushkevich (D–R) model.

The Langmuir isotherm model is based on the following assumptions: a binding site could only be occupied by one solute, there is no movement of adsorbed molecules on adsorbent surface plane, all sites have the same energy levels, and accumulation of adsorbed solute is up to monolayer coverage [20]. The Langmuir equation is described as follows:

$$\frac{C_e}{q_e} = \frac{C_e}{q_L} + \frac{1}{q_L b} \tag{6}$$

where q_L is the maximum adsorption capacity at monolayer coverage (mg/g) and b is the Langmuir equilibrium constant (mL m^{-1} g^{-1}).

The Freundlich model is a widely used empirical equation that describes adsorption on active sites with heterogeneous energy distributions [13,21]. It is given by the following:

$$\ln q_e = \frac{1}{n}\ln C_e + \ln K_F \tag{7}$$

where K_F is the relative adsorption capacity (mg g^{-1}) and $1/n$ (L g^{-1}) refers to the adsorption intensity.

The D–R isotherm is generally used in determining between physical and chemical adsorption. The linearized D–R equation is:

$$\ln q_e = \ln q_{D\text{-}R} - \beta\varepsilon^2 \tag{8}$$

where $q_{D–R}$ is the D–R adsorption capacity (mg g^{-1}), ε is the Polanyi potential and β is the constant related to the adsorption energy (kJ^2 mol^{-2}) [20]. The Polanyi potential, ε could be calculated using the following equation:

$$\varepsilon = RT\ln\left(1 + \frac{1}{C_e}\right) \tag{9}$$

where T is the absolute operating temperature (K) and R is the universal gas constant (kJ mol^{-1} K^{-1}).

The mean energy of adsorption, E (kJ mol^{-1}) can be computed using the equation below:

$$E = \frac{1}{\sqrt{-2\beta}} \tag{10}$$

Calculated values of Langmuir, Freundlich and D–R isotherm constants and coefficient of determination were listed in Table 3. The adsorption of Cu(II) on CCS, CCS–ECH, and CCS–EDGE could be best described using Langmuir model ($R^2 > 0.99$). The values of the maximum adsorption capacity, q_L could be arranged as follows: CCS–EDGE > CCS > CCS–ECH. In terms of Langmuir constant b, CCS–EDGE provided the highest value over CCS and CCS–ECH. The Langmuir constant b is related to the affinity of binding sites of adsorbent to Cu(II), which indicates that binding sites of CCS–EDGE provide the greatest attraction in adsorbing Cu(II) ions.

Based on the Freundlich constant n, the adsorption can be considered linear ($n = 1$), chemical ($n < 1$) or

Table 3
Langmuir, Freundlich, and Dubinin–Radushkevich (D–R) isotherm constants and coefficient of determination

Adsorbent	Langmuir			Freundlich			D–R		
	B (mL mg^{-1})	q_L (mg g^{-1})	R^2	n (L g^{-1})	K_F (mg g^{-1})	R^2	E (kJ mol^{-1})	q_{D-R} (mg g^{-1})	R^2
CCS	0.065	4.772	0.997	3.918	0.537	0.985	0.113	3.631	0.919
CCS–ECH	0.032	4.368	0.995	3.173	0.308	0.994	0.050	3.758	0.906
CCS–EDGE	0.073	7.201	0.991	2.289	0.715	0.977	0.041	4.342	0.896

physical ($n > 1$) [1]. The n values of CCS, CCS–ECH, and CCS–EDGE are greater than 1, which implies that the uptake of the three adsorbents is governed by physical adsorption. In addition, the parameter n indicates the favorability of the adsorbent. If $n < 1$, it implies the adsorption intensity is good or favorable in the entire concentration range studied, while $n > 1$ indicates the adsorption intensity is favorable at high concentrations and less at lower concentrations [13]. From the results, the adsorption intensity is good over high initial concentrations. The computed K_F values are arranged in the following order: CCS–EDGE > CCS > CCS–ECH, which has a similar trend with the Langmuir q_L values.

Among the three isotherm models, D–R provided the lowest coefficient of determination values ($R^2 <$ 0.92). The mean free energy of adsorption, E describes the transfer of free energy of one mole of solute from infinity (solution) to the adsorbent surface [22]. Its value provides information about the adsorption behavior on the occurrence of physical adsorption ($E < 8$ kJ mol^{-1}), ion-exchange mechanism (8 kJ mol^{-1} < $E < 16$ kJ mol^{-1}) or chemisorption ($E > 16$ kJ mol^{-1}) [16]. The values obtained for the mean adsorption energy lie in the range of 0.05–0.113 kJ mol^{-1}, which indicates that physical adsorption predominates in the Cu(II) uptake using CCS, CCS–ECH, and CCS–EDGE.

In this study, CCS–EDGE provided higher adsorption capacity over CCS and CCS–ECH. The lowest Cu (II) uptake was observed in CCS–ECH, where ECH interconnects two chitosan chains via hydroxyl groups at C-6, leaving the amine groups to interact freely with the metal ions [22]. But ECH is composed of shorter molecular chains, where the more rigid polymeric chain of ECH causes a decrease in accessibility of binding sites and reduced affinity of Cu(II) toward the basic centers of CCS–ECH [23]. On the other hand, EGDE molecules interact with chitosan via its amine groups. However, its higher adsorption capacity is attributed to EDGE having a longer molecular chain that contains two hydroxyl groups along its structure [24].

3.6. Desorption study

Desorption studies were carried out to determine the reusability of adsorbents, where the results are shown in Table 4. The recovery of Cu(II) was observed to increase as the solution becomes more acidic.

High values of desorbed Cu(II) were obtained using HCl (pH 1.0), where CCS provided better recoverability of Cu(II) in comparison with CCS–ECH and CCS–EDGE. Meanwhile, a decrease in desorption values was observed using HCl solution (pH 3.0). On the other hand, desorption using tap water (pH 7.0) provided the lowest recovery of Cu(II) for CCS, CCS–ECH, and CCS–EDGE, which indicates the stability of adsorbed Cu(II) under neutral conditions.

3.7. Adsorption study from real groundwater

Fig. 3 illustrated the percent (%) removal of Cu(II) using CCS, CCS–ECH and CCS–EDGE from real groundwater. An increase in adsorbent mass caused an increase in % Cu(II) removal. The highest Cu(II) removal using CCS, CCS–ECH, and CCS–EDGE was

Table 4
Desorption of Cu(II) from CCS, CCS–ECH, and CCS–EDGE using HCl (pH 1.0 and pH 3.0) and tap water

pH	Cu(II)	CCS (%)	CCS–ECH (%)	CCS–EDGE (%)
7.0	100	14.9	3.5	2.7
	500	11.9	9.3	7.0
	1,000	20.6	12.2	10.8
	2,000	15.7	17.5	10.5
3.0	100	22.5	17.1	13.9
	500	37.9	16.7	13.5
	1,000	21.4	18.1	13.5
	2,000	29.6	17.5	13.3
1.0	100	92.8	93.1	90.2
	500	98.3	92.1	77.5
	1,000	94.4	94.4	83.2
	2,000	98.3	87.5	83.5

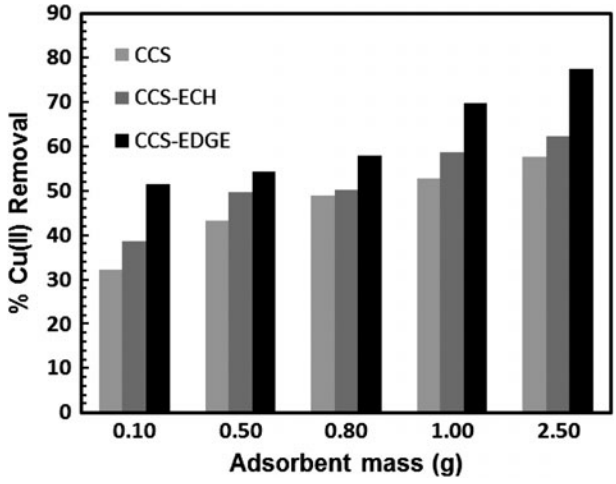

Fig. 3. Percent (%) removal of Cu(II) from real groundwater under varying adsorbent mass using CCS, CCS–ECH, and CCS–EDGE with initial Cu(II) concentration of 5 mg L^{-1}.

obtained at 57.4, 62.4, and 77.5% using 2.5 g adsorbent. The maximum adsorption capacity of CCS, CCS–ECH, and CCS–EDGE are 1.56, 2.54, and 2.98 mg g^{-1}, respectively.

The removal of Cu(II) in real groundwater is low, which is due to the interference of ionic species present in groundwater such as Fe^{2+}, $FeOH^{+}$, Mn^{2+}, and $ZnOH^{+}$ that could compete for the binding sites of the adsorbents. The other species present in the groundwater such as chloride, sulfate, phosphate, arsenite, and organic matter (humic acid) are negatively charged, which would also compete for the binding sites on CCS, CCS–ECH, and CCS–EDGE. It should be noted that the effect of the negatively charged species is not as significant as that of the positively charged species. At groundwater pH of 8.1, almost all amine groups are deprotonated ($–NH_2$), which would exert a repulsive force on the negatively charged species present in the groundwater. On the other hand, positively charged species such as Ca^{2+}, Na^{+}, and K^{+} have no significant effect on the adsorption of Cu(II) and do not compete for binding sites since chitosan does not adsorb any alkaline and alkaline earth metals.

4. Conclusion

In this study, Cu(II) removal using CCS, CCS crosslinked using ECH (CCS–ECH) and EGDE (CCS–EDGE) from aqueous solution was investigated. The effect of pH on the adsorption capacity was examined, where the maximum Cu(II) uptake for CCS and CCS–EDGE occurred at pH 5.0, while the maximum adsorption capacity of CCS–ECH was observed at pH 4.0. The pseudo-second-order equation showed to be the best fit for the kinetic data, while the equilibrium data correlated well with the Langmuir model. The adsorption of Cu(II) onto CCS, CCS–ECH, and CCS–EDGE is a combination of physical and chemical adsorption, as based on the kinetics and equilibrium study. In general, physical adsorption is the governing mechanism in the system, while chemical adsorption is the slowest adsorption step taking place. CCS–EDGE (7.20 mg g^{-1}) provided the highest adsorption capacity over CCS (4.77 mg g^{-1}) and CCS–ECH (4.36 mg g^{-1}). HCl solution (pH 1.0) provided the greatest desorption percentage for the adsorbed Cu (II). In the real groundwater system, the highest percent Cu(II) removal of 77.5% was attained using CCB–EGDE. Conclusively, cross-linked CCS illustrates to be a promising adsorbent in the removal of Cu(II) from aqueous solution and contaminated groundwater.

Nomenclature

b	—	Langmuir equilibrium constant, mL mg^{-1}
β	—	D–R constant related to the adsorption energy, $kJ^2\,mol^{-2}$
c_a	—	concentration of metal ions adsorbed, mg L^{-1}
c_d	—	concentration of metal ions desorbed, mg L^{-1}
C_e	—	final or equilibrium concentration of Cu(II), mg L^{-1}
C_0	—	initial Cu(II) concentration, mg L^{-1}
E	—	mean energy of adsorption, kJ mol^{-1}
K_F	—	relative adsorption capacity, mg g^{-1}
k_1	—	pseudo-first-order rate constant, min^{-1}
k_2	—	pseudo-second-order rate constant, g mg^{-1} min^{-1}
m	—	weight of the adsorbent, g
$1/n$	—	adsorption intensity, L g^{-1}
$q_{D–R}$	—	D–R adsorption capacity, mg g^{-1}
q_e	—	adsorption capacity at equilibrium, mg g^{-1}
q_L	—	maximum adsorption capacity at monolayer coverage, mg g^{-1}
q_t	—	adsorption capacity at time t, mg g^{-1}
R	—	universal gas constant, kJ mol^{-1} K^{-1}
t	—	contact time, min
T	—	absolute operating temperature, K
v	—	volume of Cu(II) solution, mL

References

[1] C.O. Ijagbemi, M.H. Baek, D.S. Kim, Montmorillonite surface properties and sorption characteristics for heavy metal removal from aqueous solutions, J. Hazard. Mater. 166 (2009) 538–546.

[2] C.M. Futalan, C.C. Kan, M.L. Dalida, K.J. Hsien, C. Pascua, M.W. Wan, Comparative and competitive adsorption of copper, lead, and nickel using chitosan immobilized on bentonite, Carbohydr. Polym. 83 (2011) 528–536.

[3] B. Guan, W. Ni, Z. Wu, Y. Lai, Removal of Mn(II) and Zn(II) ions from flue gas desulfurization wastewater with water-soluble chitosan, Sep. Purif. Technol. 65 (2007) 269–274.
[4] A. Kamari, W.S. Wan Ngah, Isotherm, kinetic and thermodynamic studies of lead and copper uptake by H_2SO_4 modified chitosan, Colloids Surf. B 73 (2009) 257–266.
[5] S.R. Popuri, Y. Vijaya, V.M. Boddu, K. Abburi, Adsorptive removal of copper and nickel ions from water using chitosan coated PVC beads, Bioresour. Technol. 100 (2009) 194–199.
[6] E.I. Unuabonah, B.I. Olu-Owolabi, E.I. Fasuyi, K.O. Adebowale, Modeling of fixed-bed column studies for the adsorption of cadmium onto novel polymer-clay composite adsorbent, J. Hazard. Mater. 179 (2010) 415–423.
[7] W.S. Wan Ngah, A. Ab Ghani, A. Kamari, Adsorption behavior of Fe(II) and Fe(III) ions in aqueous solution on chitosan and cross-linked chitosan beads, Bioresour. Technol. 96 (2005) 443–450.
[8] K.S. Low, C.K. Lee, A.C. Leo, Removal of metals from electroplating wastes using banana pith, Bioresour. Technol. 51 (1995) 227–231.
[9] C.H. Weng, C.Z. Tsai, S.H. Chu, Y.C. Sharma, Adsorption characteristics of copper (II) onto spent activated clay, Sep. Purif. Technol. 54(2) (2007) 187–197.
[10] C.H. Weng, P.C. Chiang, E.E. Chang, Adsorption characteristics of Cu(II) on to industrial wastewater sludges, Ads. Sci. Technol. 19(2) (2001) 143–158.
[11] F. Qin, B. Wen, X.Q. Shan, Y.N. Xie, T. Liu, S.Z. Zhang, S.U. Khan, Mechanisms of competitive adsorption of Pb, Cu and Cd on peat, Environ. Pollut. 144 (2006) 669–680.
[12] C.H. Weng, Y.C. Wu, Potential low-cost biosorbent for copper removal: pineapple leaf powder, J. Environ. Eng. 138 (2012) 286–292.
[13] W.S. Wan Ngah, S. Fatinathan, Adsorption of Cu(II) ions in aqueous solution using chitosan beads, chitosan-GLA beads and chitosan-alginate beads, Chem. Eng. J. 143 (2008) 62–72.
[14] A.A. El-Bayaa, N.A. Badawy, A.M. Gamal, I.H. Zidan, A.R. Mowafy, Purification of wet process phosphoric acid by decreasing iron and uranium using white silica sand, J. Hazard. Mater. 190 (2011) 324–329.
[15] M.W. Wan, C.C. Kan, B.D. Rogel, M.L.P. Dalida, Adsorption of copper (II) and lead (II) ions from aqueous solution on chitosan-coated sand, Carbohydr. Polym. 143 (2010) 891–899.
[16] A.H. Chen, S.C. Liu, C.Y. Chen, C.Y. Chen, Comparative adsorption of Cu(II), Zn(II), and Pb(II) ions in aqueous solution on the crosslinked chitosan with epichlorohydrin, J. Hazard. Mater. 154 (2008) 184–191.
[17] M. Belhachemi, F. Addoun, Adsorption of red congo onto activated carbons having different surface properties: studies of kinetics and adsorption equilibrium, Desalin. Water Treat. 37 (2012) 122–129.
[18] Y.S. Ho, G. McKay, Pseudo-second order model for sorption processes, Process Biochem. 34 (1999) 451–465.
[19] B.H. Hameed, I.A.W. Tan, A.L. Ahmad, Adsorption isotherm, kinetic modeling and mechanism of 2,4,6-trichlorophenol on coconut-husk based activated carbon, Chem. Eng. J. 144 (2008) 235–244.
[20] J. Febrianto, A.N. Kosasih, J. Sunarso, Y.H. Ju, N. Indraswati, S. Ismadji, Equilibrium and kinetic studies in adsorption of heavy metals using biosorbent: a summary of recent studies, J. Hazard. Mater. 162 (2009) 616–645.
[21] M.T. Sulak, H.C. Yatmaz, Removal of textile dyes from aqueous solutions with eco-friendly biosorbent, Desalin. Water Treat. 37 (2012) 169–177.
[22] M.O. Machado, E.C.N. Lopes, K.S. Sousa, C. Airoldi, The effectiveness of the protected amino group on crosslinked chitosans for copper removal and the thermodynamics of interaction at the solid/liquid interface, Carbohydr. Polym. 77 (2009) 760–766.
[23] F.C. Wu, R.L. Tseng, R.S. Juang, A review and experimental verification of using chitosan and its derivatives as adsorbents for selected heavy metals, J. Environ. Manage. 91 (2010) 798–806.
[24] W.S. Wan Ngah, C.S. Endud, R. Mayanar, Removal of copper (II) ions from aqueous solution onto chitosan and cross-linked chitosan beads, React. Funct. Polym. 50 (2002) 181–190.